Modelling and Emulation of Solar Powered Vehicle

T.M. Thamizh Thentral, A. Geetha, S. Usha, Ayush Singh, Varoon Kannan, Kotikalapudi Kameshwari Vashini

Abstract: ***With growing energy demands, switching to renewable energy is humanity's last resort. This can be achieved only if the people are ready to switch to renewable energy, right from powering their homes to replacing their fuel cars. A solar EV provides an answer to the latter. The current requirement is an efficient and economic version of a Solar Electric Vehicle. Nowadays, there is a growing market for electric vehicles given the current scenario of global warming and the need to reduce it. Although electric vehicles have their advantages, especially in terms of traction efficiency, the major disadvantage is the shorter operating distance in comparison to a conventional vehicle. This is primarily due to the comparatively low energy density of the batteries that propel these vehicles. Hence they are apt for urban, short range purposes. For example, they may be used as taxis or as delivery vehicles. This paper focuses on the simulation of electric vehicles using a Hardware in the Loop (HiL) model of an electric vehicle traction system. The vehicle is tested under different conditions to analyze its energy consumption and other parameters.***

Keywords: Hardware in Loop Simulation, Energy Storage System (ESS), Battery Management System(BMS), Boost Converter, Buck Boost Converter, Supervisory Control and Data Acquisition (SCADA).

I. INTRODUCTON

Generating electrical energy for traction has produced a negative effect by polluting the environment. It has become necessary to replace fossil fuels with renewable energy sources such as solar, biomass, wind, hydro etc. There have been eminent advancements in solar energy based photovoltaic array and they are being widely adopted as an energy source in a lot of industries for a variety of appliances. The reasons for the success of solar energy lie in its capability to produce clean and safe energy. It is available in abundant quantities and the operating and maintenance costs for harvesting solar energy are considerably low. One drawback is the absence of the source of energy during the night. Nevertheless, developments in the battery storage systems have aided hugely to overcome this drawback. They help to ensure uninterrupted power supply to any standalone system like an electric vehicle. Although PV systems manifest reliably, a desirable power capability during steady-state operation, its dynamic response during variations in power demand is considerably slow. This further strengthens the argument of a standalone PV system to be combined with a battery storage.

In the solar vehicle presented in this paper, the configuration consists of a PV panel, a storage source which also acts as a secondary source of energy, a boost converter to connect PV panels to the DC bus, a buck-boost converter connecting the energy storage system or the ESS, to the DC bus, a maximum power point tracker (MPPT) to obtain the maximum power from the PV panel and the traction load/motor. The basic configuration of the electric vehicle is shown in Fig. 1.

HIL simulation is a technique employed in the testing and development of a system having complex processes. It replaces a physical model, by a mathematical model that represents the characteristics of the former. Such a simulation provides a constructive platform by adding the complexity of the plant under control to the test platform. By including mathematical equations such as power grid dynamics, the complex processes are taken into account during the development stage. Such a method is known as plant simulation. A device under scrutiny, such as a solar panel, interacts with a computing system to deliver real-time assessments of the response of the system. HIL provides the platform to test the system under realistic operating conditions.

II. MODELLING AND CONTROL OF THE SYSTEM

The modelling of the electric vehicle in this paper consists of five major components: solar array, maximum power point tracker, battery management system, high voltage protection and motor control.

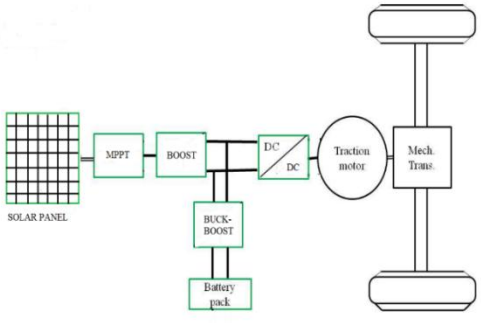

Fig.1: Basic configuration of the electric vehicle

Manuscript received January 25, 2019.

T.M. Thamizh Thentral, Assistant Professor, SRM Institute of Science and Technology, Kattankulathur, Chennai, Tamilnadu, India.

A. Geetha, Assistant Professor, SRM Institute of Science and Technology, Kattankulathur, Chennai, Tamilnadu, India.

S. Usha, Assistant Professor, SRM Institute of Science and Technology, Kattankulathur, Chennai, Tamilnadu, India.

Ayush Singh, Student, SRM Institute of Science and Technology, Kattankulathur, Chennai, Tamilnadu, India.

Varoon Kannan, Student, SRM Institute of Science and Technology, Kattankulathur, Chennai, Tamilnadu, India.

Kotikalapudi Kameshwari Vashini, Student, SRM Institute of Science and Technology, Kattankulathur, Chennai, Tamilnadu, India.

A. Modelling of Solar Array

A solar cell is a semiconductor device that converts solar energy from the sun into electrical energy by producing charges whenever a photon hits the junction. Due to various internal mechanisms, electron hole pairs are created when the cell is placed in sunlight. The number of electron pairs increases with an increase in the amount of sunlight hitting the cell.

To create a PV module and further to create an array, the cells are connected in a series and parallel arrangement. The PV cell exhibits a nonlinear I-V and P-V characteristic which varies with the intensity of radiation and the temperature of the cell as shown in Fig.2 and Fig.3.

For the purpose of modelling the solar panel we have considered a Single Diode Model (SDM) as shown in Fig. 4. This model includes a short circuit current, open circuit voltage, and an ideal diode. The effect of series and shunt resistances are also taken into consideration.

The mathematical equations that pertain to the model can be represented through quantities: the open circuit voltage (V_{oc}), the short circuit current (I_{sc}), and the maximum power point (P_{mpp}).

The short circuit current, I_{sc} is show below:

$$Isc = Ig - Irs\left[exp\left(\frac{qI_{sc}R_sN_s}{N_sKTA}\right) - 1\right] - \left(\frac{I_{sc}R_s}{R_{sh}}\right) \quad (1)$$

The current I_{mpp}, at maximum power is given as:

$$I_{mpp} = I_g - I_0\left[\left(\frac{q(V_{mpp} + I_{mpp}R_sN_s)}{N_sKTA}\right) - 1\right] - \left(\frac{V_{mpp} + I_{mpp}R_sN_s}{N_sR_{sh}}\right) \quad (2)$$

The equation for current at the open circuit point, represented as I_{oc}, is given by:

$$I_{oc} = I_g - I_o\left[exp\left(\frac{qV_{oc}}{N_sKTA}\right) - 1\right] - \left(\frac{V_{oc}}{N_sR_{sh}}\right) \quad (3)$$

It is known that at the maximum power point (MPP) the slope of the P-V curve is zero:

$$\frac{dP}{dV} = 0 \quad (4)$$

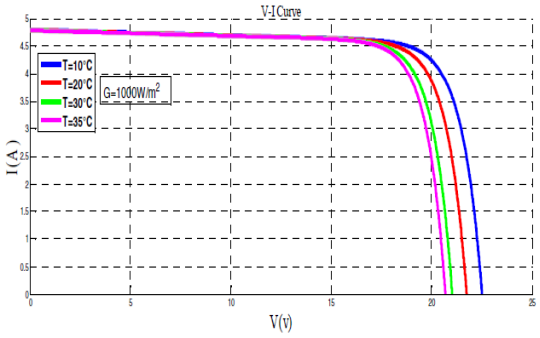

Fig.2: Influence of temperature on the V-I characteristic of the panel.

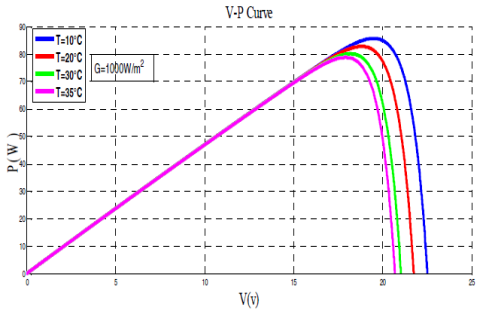

Fig. 3: Influence of temperature on the V-P characteristic of the panel.

According to eq. (1,2,3 and 4), there are four equations available and we need to find five parameters. Hence the need to use a fifth equation in order to solve the problem arises. The ratio of the derivative of the current to the derivative of the voltage at the short-circuit condition is used as the fifth equation. The shunt resistance, Rsh plays a major role in determining this condition.

$$\frac{dI}{dV}\Big|_{I=I_{sc}} = \frac{-1}{R_{sh}} \quad (5)$$

From eq. (1 and 3), we can determine the photogenerated current I_g and the saturation current I_0 as:

$$I_g = I_0\left[\exp\left(\frac{qV_{oc}}{N_sKTA}\right) - 1\right] - \left(\frac{V_{oc}}{N_sR_{sh}}\right) \quad (6)$$

The from eq. (6 and 1) we obtain:

$$I_{sc} = I_o\left[exp\left(\frac{qV_{oc}}{N_sKTA}\right) - exp\left(\frac{qI_{sc}R_sN_s}{N_sKTA}\right)\right] - \left(\frac{V_{oc} - I_{sc}R_s}{N_sR_{sh}}\right) \quad (7)$$

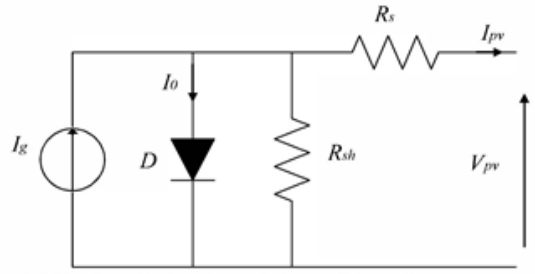

Fig. 4: PV cell modelled as a single diode circuit including R_s and R_{sh}

In the above equation, the second term in the parenthesis is trivial in comparison to the first term. Hence, we neglect it and arrive at the following equation:

$$I_{sc} = I_0\left[\exp\left(\frac{qV_{oc}}{N_sKTA}\right)\right] - \left(\frac{V_{oc} - I_{sc}R_s}{N_sR_{sh}}\right) \quad (8)$$

By rearranging and solving saturation current equation, we get:

$$I_0 = I_{sc} - \left(\frac{V_{oc} - I_{sc}R_s}{N_sR_{sh}}\right)\exp\left(-\frac{qV_{oc}}{N_sKTA}\right) \quad (9)$$

The equation for current at maximum power point is obtained by consolidating equations (2,6 and 9):

$$I_{mpp} = I_{sc} - \left(\frac{V_{mpp} + I_{mpp}R_s - I_{sc}R_s}{R_{sh}}\right) - \left(I_{sc} - \frac{V_{oc} - I_{sc}R_s}{R_{sh}}\right) exp\left(\frac{q(V_{mpp} + I_{mpp}R_s - V_{oc})}{N_sKTA}\right) \quad (10)$$

B. Mathematical Model of Dc-Dc Converter

Boost Converter

The circuit diagram of a step up operation of a DC-DC boost converter is shown in Fig.5. When the switch S_1 is closed for a time t_1, the inductor current rises and the energy is stored in the inductor. If the switch S_1 is opened for a time t_2, the energy stored in the inductor is transferred to the load through the diode D_1 as a result of which the inductor current reduces.

Published By:
Blue Eyes Intelligence Engineering
& Sciences Publication

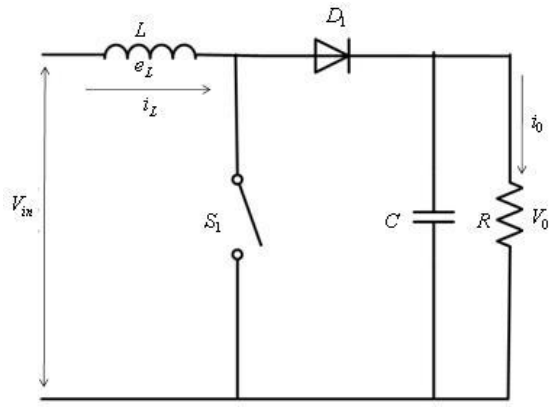

Fig. 5: Boost converter

When the switch S_1 is turned on, the voltage across the inductor is given by:

$$v_L = L\frac{di}{dt} \quad (11)$$

The peak to peak ripple current in the inductor is given by:

$$\Delta I = \frac{V_s}{L} t_1 \quad (12)$$

The average output voltage is:

$$v_0 = V_s + L\frac{\Delta I}{t_2} = V_s\left(1+\frac{t_1}{t_2}\right) = V_s\frac{1}{1-D} \quad (13)$$

From eq. (13) we infer that:

- The load voltage can be increased by altering D, which is the duty ratio.
- The least output voltage is V_s and is got when D becomes 0.
- The converter cannot be switched on continuously such that $D = 1$. Whenever the duty ratio approaches a value of one, the output becomes extremely sensitized to changes in D.

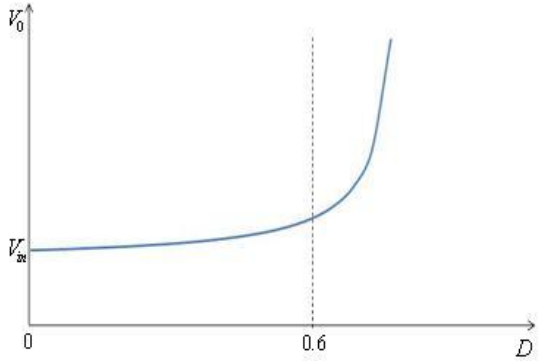

Fig. 6: Output voltage vs. Duty ratio for boost converter

Buck-Boost Converter

The general configuration of Buck-Boost converter in mode 1 and mode 2 is shown in Fig. 7 and 8. A buck-boost converter is obtained via a cascade connection of the two basic converters: the step-down converter and the step-up converter.

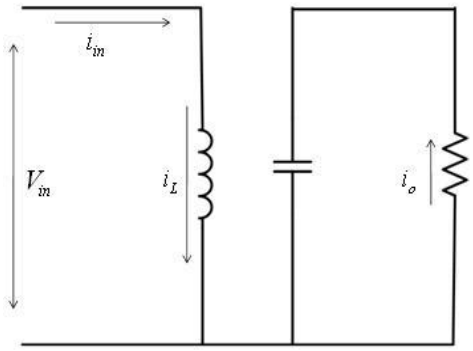

Fig. 7: Buck-Boost converter in mode 1

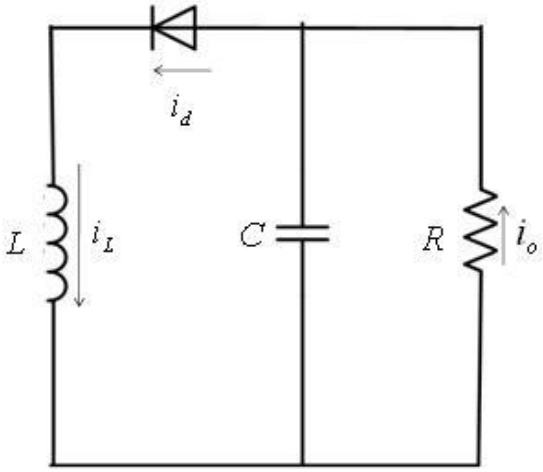

Fig. 8: Buck-Boost converter in mode 2

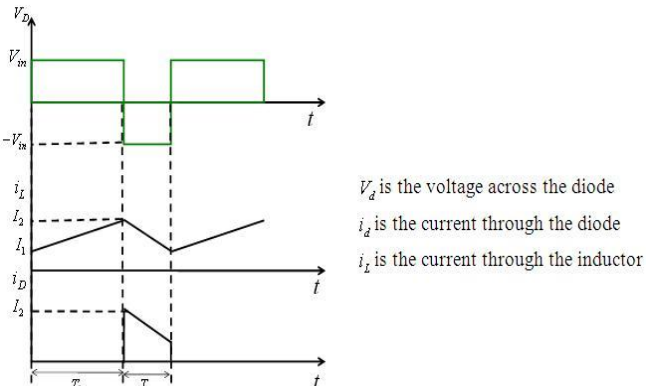

Fig. 9: Current and voltage waveforms of buck-boost converter.

The working and operation of the circuit is divided into two modes: In mode 1, the switch S_1 is turned on and the diode D is reversed biased. Here, the input current rises and flows through inductor L and switch S_1. In mode 2, the switch S_1 is off and the current, which originally was flowing through the inductor, flows through L, C, D and load . In this mode the energy contained in the inductor (L) is transferred to the load and the inductor current (i_L) starts to reduce until the switch S_1 is turned on again in the next cycle.The waveforms for the steady-state voltage and current are shown in Fig. 9.

The current through the inductor (L) rises linearly since the frequency of switching is taken to be high. Thus, the relation between the voltage and current in mode 1 is:

$$V_{in} = L\frac{I_2 - I_1}{T_1} = L\frac{\Delta I}{T_1}$$

$$\Rightarrow T_1 = L\frac{\Delta I}{V_{in}} \quad (14)$$

In mode 2, and in a time T_2 the inductor current falls linearly from I_2 to I_1. It is given by:

$$V_o = -L\frac{\Delta I}{T_2}$$

$$\Rightarrow T_2 = -L\frac{\Delta I}{V_o} \quad (15)$$

The peak to peak ripple current through the inductor in mode 1 and 2 is denoted as $\Delta I (= I_2 - I_1)$. From eq.(14) and eq.(15) the relation between the input and output voltage is obtained as

$$\Delta I = \frac{V_{in}T_1}{L} = -\frac{V_o T_2}{L} \quad (16)$$

The relation between the on and off time, of the switch S_1, and the total time duration is expressed in terms of duty ratio (D) as:

$$T_1 = DT \quad (17)$$

$$T_2 = (1-D)T \quad (18)$$

Substituting the values of T_1 and T_2 from eq.(17) and eq.(18) into eq.(16)gives:

$$V_o = -\frac{V_{in}D}{1-D} \quad (19)$$

If the converter is assumed to be lossless, then

$$V_{in}I_{in} = -V_o I_o$$

$$V_{in}I_{in} = \frac{V_{in}D}{1-D}I_o \Rightarrow I_{in} = \frac{I_o D}{1-D} \quad (20)$$

The switching period T obtained from eq. (14) and eq. (15) as:

$$T = T_1 + T_2 = L\frac{\Delta I}{V_o} - L\frac{\Delta I}{V_{in}} = L\Delta I\frac{(V_{in} - V_o)}{V_{in}V_o} \quad (21)$$

The peak to peak ripple current $\Delta I$is obtained from eq.(21) as:

$$\Delta I = \frac{TV_{in}V_o}{L(V_o - V_{in})} = \frac{DT}{L}V_{in} = \frac{V_{in}D}{fL} \quad (22)$$

where, f is the controlling frequency.

When the switch S_1 is turned on , the filter capacitor provides the load current for a time duration T_1. The average discharge current of the capacitor $I_{cap} = I_{out}$, and the peak to peak ripple current of the capacitor is:

$$\Delta V_{cap} = \frac{1}{C}\int_0^{T_1} I_{cap}dt = \frac{1}{C}\int_0^{T_1} I_o dt = \frac{I_o T_1}{C} = \frac{I_o D}{fC} \quad (23)$$

C. Electric Motor

A permanent magnet (PM) motor is a motor which does not possess a field winding on the stator frame to provide the magnetic field required for induction. Instead it depends upon permanent magnets for the magnetic field against which the rotor field interacts to produce torque. Cost is a critical aspect for the success of any device. Hence there arises a need for developing low cost and more efficient permanent magnets.PM motors have demonstrated higher efficiency and also require lesser amounts of current to avail the same torque as the other motors. The challenges for motors in an electric vehicle is expressed in terms of efficiency, speed range, weight, torque and lifetime.

By applying Newton's second law of motion, the acceleration of the vehicle can be shown as [12]:

$$\frac{dV}{dt} = \frac{\sum F_t - \sum F_{resistance}}{\delta M} \quad (24)$$

where, V is the speed of the vehicle, $\sum F_t$ is the net tractive effort, $\sum F_{resistance}$ is the total resistance, M is the total mass of the vehicle and δ is the mass factor for converting the rotational inertias of rotating components into translational mass.

The torque that is generated is given as follows:

$$T_g = \frac{9.55P_w}{n} \quad (25)$$

where, T_g is the total torque, P_w is power of the motor and n is the speed of the motor.

The required torque is:

$$T_r = Fr \quad (26)$$

D. Battery and Battery Management System

Lithium battery is light and its unit-level shape (prismatic, cylindrical and pouch) helps pack assembly easily structured with a stacking design method so that its energy density relatively higher than Ni-MH and Lead-acid batteries have.

Nevertheless, the Lithium-Ion battery systems still have several technical issues to improve. Lithium-Ion battery requires more complex management systems to operate safely and to expand lifecycles. So this requirement makes Battery Management System (BMS) strictly control the battery power. In case of an abnormal situation, some cases need to be disconnected with the high voltage battery power. But, if the battery power is disconnected, the electric vehicle, which is distinct from hybrid electric vehicles, doesn't have the second operating mode such as a diesel mode. Hence the driver of the vehicle driver would find himself in a hazardous position. For example, in case the communication to monitor unit cell voltages is not working, BMS cannot measure cell voltages at the moment. This means that the BMS cannot decide whether the battery is over-charged or not. So it would disconnect high voltage switches thereby cutting off supply of battery power to the motor and also to prevent charging power from the generator. On a highway this situation could cause vehicle accidents.

Basically a battery cell voltage is monitored online. When the monitored cell voltage reaches the operating boundaries, both upper and lower boundaries, a protection alarm is turned on to give a caution to the driver. In case of voltage monitoring. communication is working without any abnormality, the cell voltages can be estimated with a battery model and battery characteristics including State-of-Charge (SOC),Open Circuit Voltage (OCV).

The most popular Li-Ion battery model is shown below.

Published By:
Blue Eyes Intelligence Engineering
& Sciences Publication

The first order electric equivalent circuit with an ohmic resistance, R_i and one set of resistance, R_d and capacitance, C_d in parallel (Fig. 11).

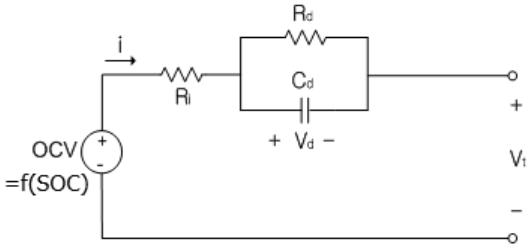

Fig. 10: The first order electric equivalent circuit model

Based on the battery model mentioned above, BMS can now draw the outline of the cell voltage for estimating, Eq. (27-1). OCV can be converted by SOC calculated only with the current value, Eq. (27-2). DC-IR is also one of battery characteristics, the battery has its own values Eq. (27-3).

$$V_t = OCV - i \times (DCIR) \quad (1)$$

$$OCV = f(SOC_n) = f(SOC_{n-1} + \frac{\int I dt}{Q}) \quad (2)$$

$$DCIR = R_i + R_d = f(SOC, T, t) \quad (3)$$

$$V_t < V_{high} \text{ OR } V_t > V_{low} \quad (4) \qquad (27)$$

E. Maximum Power Point Tracker

As the amount of radiation affects the PV characteristics, an MPPT control technique is required for tracking the optimal operating point of maximum power. The effect of radiation on the PV characteristic leads to the introduction of an operating point change. Hence, the MPPT control technique is employed. A variety of MPPT control methods have been in use. In this paper, we focus on the Fractional Open-Circuit Voltage (FOV) and Fractional Short-Circuit Current (FSC) approaches.

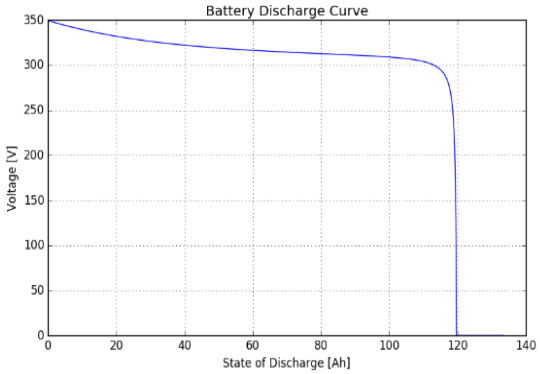

Fig. 11: Battery discharge curve

F. Fractional Open-Circuit Voltage Method

The algorithm in FOV is expressed via a linear relationship between the open circuit voltage V_{oc} and the optimal voltage, V_{mpp}.The relationship between the two parameters is as shown:

$$V_{mpp} = K_v V_{oc} \quad (28)$$

where K_v is a constant factor, varying between 0.73 and 0.8. The introduction of a static switch into the PV process is essential for the purpose of measuring the open circuit voltage.

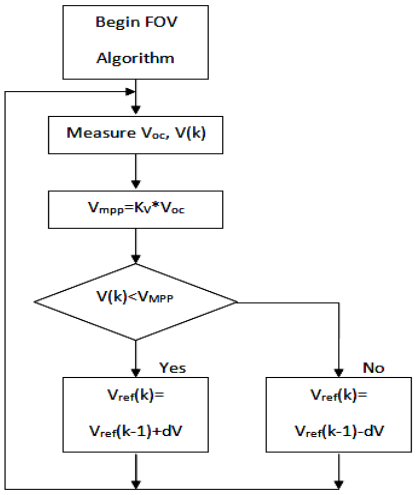

Fig. 12: Flowchart of the FOV method.

G. Fractional Short-Circuit Current Method

The Fractional Short Circuit uses the proportionality relationship between the short-circuit current I_{cc} and the optimal current I_{mpp}.The relationship between the two quantities is as shown:

$$I_{mpp} = K_i I_{cc} \quad (29)$$

where K_i is a constant factor which varies between 0.85 and 0.92 [17].

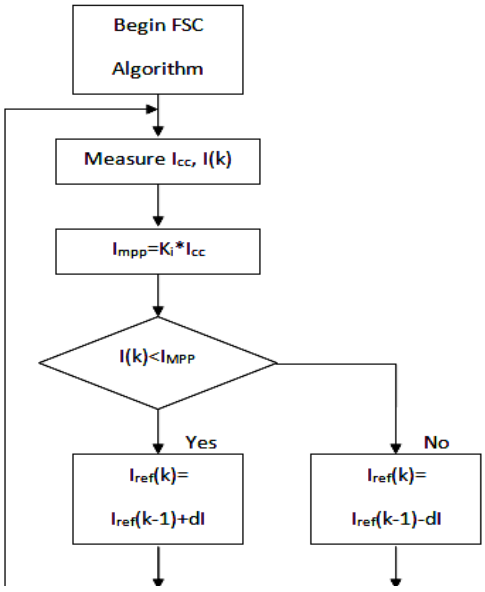

Fig. 13: Flowchart depicting the FSC method.

The FSC method requires short circuit measurements. Hence a static switch is connected in parallel to the PV process to obtain these measurements.

III. SIMULATION RESULTS

Initially we provide the dc machine specifications such as load type, load source, load coefficient, etc. as shown in Fig. 14. After script initialization, the simulated values such as the battery emf, electric and mechanical torque, and mechanical speed results are shown in the scope (shown in Fig. 15).

The voltage (V) -current (I) curve is plotted according to the provided output specifications as shown in Fig. 16, the corresponding power produced is calculated from it, and also the efficiency of the motor can be calculated. Fig 17 shows the level of machine mechanical torque, electrical torque, battery level and other value readings from the dc motor machine.

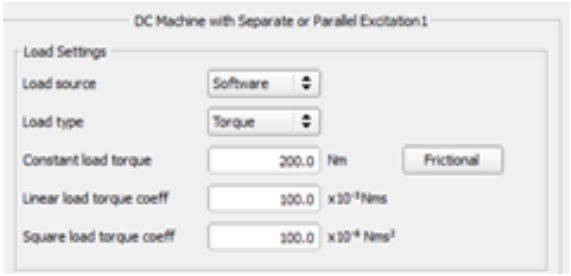

Fig. 14: Script Initialisation

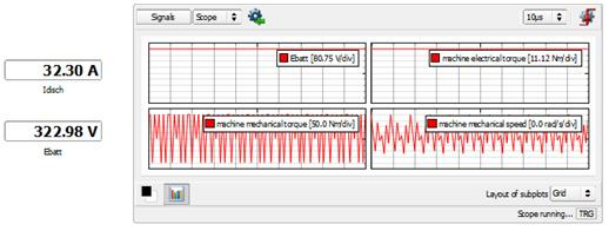

Fig. 15: Graph depicting battery e.m.f., electrical torque, mechanical torque and speed

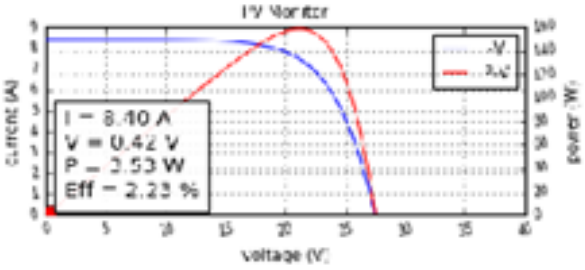

Fig. 16: V-I curve with corresponding power

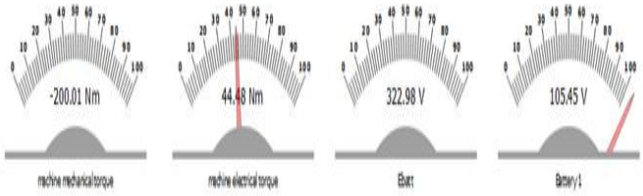

Fig. 17: Values for mechanical torque, electrical torque, battery level

IV. CONCLUSION

The energy consumption and the electrical power needed for different electric drives can be studied by employing a HIL setup. The use of a HIL setup results in scaling factors, and these factors are used to generate various simulations to test the performance and efficiency of electric drives, among other things in any given vehicle. Using the scaling method in union with the HIL setup presented, the energy consumption of different electric vehicle setups can be simulated without changing the setup itself. As this method is independent of the used HIL setup, it can be applied to other laboratory setups.

REFERENCES

1. D. Maclay, "Simulation gets into the loop," *IEE Review*, vol. 43, no. 3,pp. 109–112, 1997.
2. C. Dufour, V. Lapointe, J. Belanger, and S. Abourida, "Hardware-in-the loop closed-loop experiments with an FPGA-based permanent magnet synchronous motor drive system and a rapidly prototyped controller," in *Proc. IEEE Int. Symp. Industrial Electronics ISIE 2008*, pp. 2152–2158,2008.
3. S. Abourida and J. Belanger, "Real-time platform for the control, prototyping, and simulation of power electronics and motor drives, "in *Proc. 3rd International Conference on Mondeling, Simulation, and Applied Optimization*, 2009.
4. C. Bordas, C. Dufour, and O. Rudloff, "A 3-level neutral-clamped inverter model with natural switching mode support for the real-time simulation of variable speed drives," in *Planet-RT Opal White Paper*,2009.
5. G. G. R. Walker, Evaluating MPPT converter topologies using amatlab PV model, Journal of Elect. Electron. Eng. , vol. 21, pp.49-55,2001.
6. N. Jeddi, L. El Amraoui, Design of a photovoltaic system for constant output voltage and current, The Fifth International Renewable Congress, pp. 586-591, Hammet, Tunisia, March ,2014.
7. N. Hatziargyriou et. All, Modeling New Forms of Generation and Storage, CIGRE Technical Brochure, 2000.
8. M. G. Villalva, 1 R. Gazoli, and E. R. Filho, Comprehensive approach to modeling and simulation of photovoltaic arrays, IEEE Transaction on Power Electronics, vol. 24, no. 5, pp.1198-1208, May 2009.
9. H. Tian, F. Mancilla-David, K. Ellis, E. Muljadi, and P. Jenkins, A cell-to-module-to-array detailed model for photovoltaic panels, Solar Energy, vol. 86, no. 9, pp. 2695-2706, September2012.
10. I. Husain, *Electric and Hybrid Electric Vehicles*, CRC Press, 2003
11. B. Dunn, H. Kamath and J. Tarascon, "Electrical Energy Storage for the Grid: A Battery of Choices", Science 18 Nov 2011, Vol. 334, Issue6058, pp. 928-935, 2011
12. Davide Cittanti, Alessandro Ferraris, AndreaAirale, Sabina Fiorot, Santo Scavuzzo and Massimiliana Carello, "Modeling Li-ion batteries for automotive application: A trade-off between accuracy and complexity", IEEE International Conference of Electrical and Electronic Technologies for Automotive, pp. 1-8, 2017
13. J. Surya Kumari, Ch. Sai Babu, *"Comparison of Maximum Power Point Tracking Algorithms for Photovoltaic System"*, IJAET, Vol. 1, Issue 5, pp.133-148, Nov 2011.
14. M. H. Rashid, *Power Electronics: Circuits, Devices and Applications*, 3rd edition, Pearson, 2004 [15] V. R. Moorthi, *Power Electronics: Devices, Circuits and Industrial Applications*, Oxford University Press, 2007
15. Hairul Nissah Zainudin, Saad Mekhilef, **"***Comparison Study of Maximum Power Point Tracker Techniques for PSystems"*,MEPCON'10, Cairo University, Egypt, December 2010.
16. Burri Ankaiah, Jalakanuru Nageswararao, *"Enhancement of Solar Photovoltaic Cell by Using Short-Circuit Current Mppt Method"*, IJESSI, Volume 2 Issue 2,PP.45-50, February 2013.